

Site preference of U and Th in Cl, F, and Sr apatites

YUN LUO,^{1,*} JOHN M. HUGHES,^{1,2} JOHN RAKOVAN,¹ AND YUANMING PAN³

¹Department of Geology, Miami University, Oxford, Ohio 45056, U.S.A.

²Office of the Provost, University of Vermont, Burlington, Vermont 05405, U.S.A.

³Department of Geological Sciences, University of Saskatchewan, Saskatoon, Saskatchewan S7N 5E2, Canada

ABSTRACT

Crystals of U- and Th-doped fluor-, chlor-, and strontium-apatite have been synthesized from phosphate-halide-rich melts, and their structures were refined at room temperature with single-crystal X-ray diffraction intensities to $R = 0.0167\text{--}0.0255$. Structure refinements of U-doped fluorapatites indicate that U substitutes almost exclusively into the Ca2 site with site occupancy ratios $U_{\text{Ca}2}/U_{\text{Ca}1}$ that range from 5.00 to 9.33. Similarly, structure refinements of Th-doped fluorapatites indicate that Th substitutes dominantly into the Ca2 site with $\text{Th}_{\text{Ca}2}/\text{Th}_{\text{Ca}1}$ values that range from 4.33 to 8.67. Structure refinements of U-doped chlorapatites show that U is essentially equally distributed between the two Ca sites with $U_{\text{Ca}2}/U_{\text{Ca}1}$ values that range from 0.89 to 1.17. Results for Th-doped chlorapatites show that Th substitutes into both Ca1 and Ca2 sites with $\text{Th}_{\text{Ca}2}/\text{Th}_{\text{Ca}1}$ values that range from 0.61 to 0.67. In the Th-doped strontium-apatites with F and Cl end-members, Th is incorporated into both the Ca1 and Ca2 sites. The range of $\text{Th}_{\text{Ca}2}/\text{Th}_{\text{Ca}1}$ values is 0.56 to 1.00 for the F end-member, and 0.39 to 0.94 for the Cl end-member. XANES measurements of the U-doped samples indicate that U in fluorapatite is tetravalent, whereas in chlorapatite it is heterovalent but dominantly hexavalent.

According to our calculation, the volume of the Ca2 polyhedron increases by about 5.8% from fluorapatite to chlorapatite, but that of Ca1 polyhedron increases by only 0.59%. We speculate that the much greater size of the Ca2 polyhedron in chlorapatite may diminish the selectivity of this position for U and Th. The incorporation of U and Th into fluorapatite results in a decrease in the size of both Ca polyhedra, but the incorporation of U and Th into chlorapatite results in an increase in the volume of both Ca polyhedra. We suggest that the preference of U and Th for both Ca sites in chlorapatite is attributable to the large increase in size and distortion of the Ca2 polyhedron upon substitution of Cl for F.

Keywords: Apatite, uranium, thorium, single-crystal XRD, uranium XANES in apatite

INTRODUCTION

The crystal chemistry of trace metals in the apatite-group minerals, $\text{Ca}_5(\text{PO}_4)_3(\text{F},\text{OH},\text{Cl})$, is of considerable significance in geology, biology, materials, and environmental sciences. Apatite can accommodate numerous substituents, including many radionuclides of environmental concern. Monovalent (Na^+ , K^+), divalent (Sr^{2+} , Pb^{2+} , Ba^{2+} , Mn^{2+} , Cd^{2+}), trivalent (REE $^{3+}$), tetravalent (Th $^{4+}$, U $^{4+}$), and hexavalent cations (U $^{6+}$) have been reported to substitute into Ca sites in the apatite structure (Pan and Fleet 2002). Up to 15.85 wt% ThO_2 and 2.88 wt% UO $_2$ have been reported as substituents in natural apatite structures, especially in the REE-rich varieties (Della Ventura et al. 1999; Oberti et al. 2001). Although scores of studies have focused on the crystal chemistry of substituents in apatite, little is known about the mechanism of incorporation and the structural response of apatite to substituent U and Th, despite the extensive use of those elements in geochronological and petrogenetic studies for over half a century (Larsen et al. 1952; Altschuler et al. 1958; Oosthuizen and Burger 1973). Because of apatite's high affinity for U and Th, its thermal annealing properties, and its relatively low solubility in most surface environments, there is great interest

in apatite as a solid nuclear waste form and a contaminant sequestration agent (Chen et al. 1997a, 1997b; Carpene and Lacout 1998; Conca and Wright 1998; Bostick et al. 1999; Ewing and Wang 2002; Carpene et al. 2003; Knox et al. 2003; Conca et al. 2006; Raicevic et al. 2006). Rakovan et al. (2002) reported the structural characterization of U $^{6+}$ in apatite as the first step in the investigation of U and Th in the apatite structure. Considerable work remains to characterize the structural response of apatite to substituent U and Th.

The structure of apatite was determined more than a half century ago (Mehmel 1930; Náray-Szabó 1930). Hughes et al. (1989) reported the most recent structure refinements on natural near-end-member fluorapatite, chlorapatite, and hydroxylapatite. There are two Ca polyhedra in the apatite structure that are hexagonally disposed about a central [001] hexad (Hughes and Rakovan 2002). Ca1 is coordinated to nine O atoms ($3 \times \text{O}1$, $3 \times \text{O}2$, $3 \times \text{O}3$; Fig. 1) in a tricapped trigonal prism. Ca2 bonds to six O atoms ($\text{O}1$, $\text{O}2$, $4 \times \text{O}3$) and one column anion ($\text{X} = \text{F}, \text{Cl}, \text{OH}$; Fig. 1). The two Ca positions in apatite offer quite different stereochemical environments and are able to accommodate a variety of cations as substituents (Fleet et al. 2000).

Understanding the site preference and the structural response of apatite to U and Th substituents will help explore the mechanism of radionuclide retention and release in apatite, which is

* E-mail: luoy1@muohio.edu

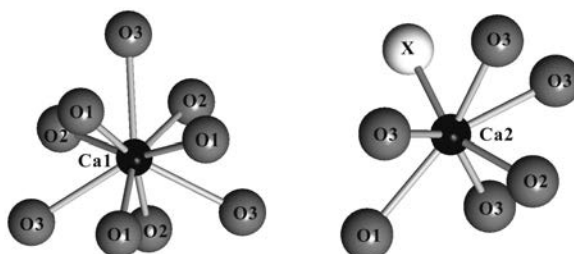


FIGURE 1. Nearest neighbor environment of the two Ca sites in the apatite structure. Left is the Ca1 polyhedron, right is the Ca2 polyhedron.

of importance in the design and evaluation of apatite as a solid nuclear waste form. Furthermore, it is of significance for use of U-Th-containing apatites in petrologic and geochronological studies. In an EXAFS study, Rakovan et al. (2002) found U^{6+} substitutes into the Ca1 site in apatite synthesized at 1350 °C. The substitution causes a decrease in the Ca1-O1 and Ca1-O2 bond lengths and EXAFS data indicate a weaker Ca1-O3 interaction. They also speculated that a likely distortion is the rotation of O1 and O2 triads to approximate an octahedral geometry around U^{6+} . We present here direct observation of U and Th substitution into apatite, investigations of the site preference, and the structural responses to these substituents in a series of synthetic fluor-, chlor-, and strontium-apatite crystals.

EXPERIMENTAL METHODS

Sample synthesis

Single crystals of U- and Th-doped fluor-, chlor-, and strontium-apatite were grown from phosphate-halide-rich melts by use of a modified flux method (Prener 1967; Pan et al. 2003; Nokhrin et al. 2005). The starting mixtures for the synthesis of U-doped fluorapatite (UFAP), U-doped chlorapatite (UCIAP), Th-doped fluorapatite (ThFAP), Th-doped chlorapatite (ThCIAP), Th-doped strontium-fluorapatite (ThSrFAP), and Th-doped strontium-chlorapatite (ThSrCIAP) were $\text{Ca}_5(\text{PO}_4)_3\text{F-CaF}_2-\text{UO}_2-\text{SiO}_2-\text{NaF}$, $\text{Ca}_5(\text{PO}_4)_3(\text{OH})-\text{CaCl}_2-\text{UO}_2-\text{SiO}_2$, $\text{Ca}_4(\text{PO}_4)_3\text{F-CaF}_2-\text{ThO}_2-\text{SiO}_2$, $\text{Ca}_5(\text{PO}_4)_3(\text{OH})-\text{CaCl}_2-\text{ThO}_2-\text{SiO}_2$, $\text{Sr}_5(\text{PO}_4)_3\text{F-SrF}_2-\text{ThO}_2-\text{SiO}_2$, and $\text{Sr}_5(\text{PO}_4)_3\text{Cl-SrCl}_2-\text{ThO}_2-\text{SiO}_2$, respectively. These mixtures (~100 mg each), containing ~15 wt% UO_2 or ThO_2 , were made from high-purity chemicals obtained from the Sigma-Aldrich Chemical Company and were sealed in platinum capsules by welding. All six experimental runs were carried out in a Thermolyne 46100 muffle furnace equipped with a programmable controller, at the Department of Geological Sciences, University of Saskatchewan. The three runs producing fluorapatite (UFAP, ThFAP, and ThSrFAP) were first heated to 1375 °C and held there for 24 h to ensure complete melting and homogenization, and were then cooled to 1220 °C at the rate of 2 °C/h and then quenched in water. The three runs producing chlorapatite (UCIAP, ThCIAP, and ThSrCIAP) were first heated to 1280 °C and held there for 10 h, and then cooled to 1060 °C at the rate of 2 °C/h and quenched in water.

Chemical analysis

Each of the synthetic samples was prepared for electron microprobe analysis (EMPA). The samples were first examined by SEM using backscattered electron imaging and EDS analysis. Because of the typically small grain size (approximately 40–100 µm), specialized sample preparation procedures were employed following the description by Dunbar et al. (2003). Data were collected with a Cameca SX-100 electron microprobe at the New Mexico Bureau of Mines and Resources, Socorro, New Mexico. The microprobe was operated at 15 kV and 19.9 nA. Beam size used was 10 µm. Elements analyzed (and standards used) include Ca (fluorapatite), Sr (synthetic SrTiO_3), Na (albite), P (fluorapatite), Si (orthoclase), U (UO_2), Th (ThO_2), F (fluorapatite), and Cl (scapolite). Table 1 gives the compositional data for all of the samples.

TABLE 1. Chemical analyses of U- and Th-doped fluor-, chlor-, and strontium-apatite

Apatite	UFAP	UCIAP	ThFAP	ThCIAP	ThSrFAP	ThSrCIAP
P_2O_5 (wt%)	41.53	37.68	41.41	34.84	26.12	26.31
SiO_2	0.26	2.57	0.56	3.31	0	0
ThO_2	0.01	0.12	1.79	4.61	1.67	0.01
UO_2	2.00	1.03	0	0.02	0	0
CaO	53.73	52.20	53.65	51.66	0.21	0.22
SrO	0.01	0.07	0.02	0.09	67.81	67.10
Na_2O	0.18	0.01	0.04	0.02	0.01	0
F	3.10	0.65	2.38	0.06	2.97	0.01
Cl	0.02	5.64	0	5.39	0.01	4.57
$\text{O} = \text{F, Cl}$	1.31	1.55	1.00	1.24	1.18	1.04
Total	99.53	98.42	98.85	98.76	97.44	97.18

Chemical formulae based upon 26 anions						
P	6.02	5.64	6.04	5.38	5.75	5.87
Si	0.04	0.45	0.10	0.60	—	—
Th	—	—	0.07	0.19	0.10	0.001
U	0.08	0.04	—	—	—	—
Ca	9.85	9.88	9.91	10.10	0.06	0.06
Sr	—	0.01	—	0.01	10.22	10.25
Na	0.06	—	0.01	0.01	0.01	—
O	24.32	23.95	24.70	24.30	23.70	23.95
F	1.68	0.36	1.30	0.03	2.29	0.01
Cl	0.01	1.69	—	1.67	—	2.04
OH^*	0.32	—	0.70	0.30	—	—

* OH calculated from $\text{F} + \text{Cl} + \text{OH} = 2$.

Crystal structure refinements

X-ray diffraction data were collected in triplicate on separate single crystals from each sample, with concordant results; the data from the structures with the lowest R values are reported. Crystals were chosen after screening by SEM using backscattered electron imaging and EDS analysis to avoid intergrowths with other phases. Single crystal measurements were made at room temperature with a Bruker Platform goniometer equipped with an APEX 4K CCD detector and $\text{MoK}\alpha$ radiation, for a full sphere of data comprising 4500 frames collected at a detector distance of 5.04 cm, with 0.2° frame width. The measured intensities were corrected for Lorentz and polarization effects using the program SAINT and an empirical absorption correction was applied using the program SADABS (Bruker 1997). The structures were routinely refined from the apatite starting model (Hughes et al. 1991) in space group $P6_3/m$ using the Bruker SHELXTL version 6.10 package of programs, with neutral-atom scattering factors and terms for anomalous dispersion. Refinements were performed with anisotropic thermal parameters for all non-hydrogen atoms, and the structures were refined on F^2 . Experimental details and crystal data of structure refinements are given in Table 2, and in Table 3 we list the atom parameters. Table 4 presents selected interatomic distances. Tables 6¹ and 7¹ contain anisotropic thermal parameters and observed and calculated structure factors, respectively.

XANES measurements

Uranium L_3 -edge XANES measurements were conducted at the beamline X27A of the National Synchrotron Light Source, Brookhaven National Laboratory, U.S.A. The X-ray storage ring operated at 2.8 GeV with a maximum current of 280 mA. A monochromator with a water-cooled channel cut Si (111) crystal was used to select the desired X-ray energy. The X-ray beam was focused to about 10 µm vertically and 15 µm horizontally by a focusing system that consists of two 20 cm long, dynamically bent rhodium-coated silicon mirrors arranged in Kirkpatrick-Baez (KB) geometry. The measurements were made in fluorescence mode using a Canberra 13-element germanium array solid-state X-ray detector

¹ Deposit item AM-09-008, Tables 6 and 7 anisotropic thermal parameters and observed and calculated structure factors, respectively. Deposit items are available two ways: For a paper copy contact the Business Office of the Mineralogical Society of America (see inside front cover of recent issue) for price information. For an electronic copy visit the MSA web site at <http://www.minsocam.org>, go to the American Mineralogist Contents, find the table of contents for the specific volume/issue wanted, and then click on the deposit link there.

TABLE 2. Experimental details and crystal data of structure refinements

	UFAP	UCIAP	ThFAP	ThCIAP	ThSrFAP	ThSrCIAP
Space group	$P6_3/m$	$P6_3/m$	$P6_3/m$	$P6_3/m$	$P6_3/m$	$P6_3/m$
a (Å)	9.3709(2)	9.6233(2)	9.375(2)	9.6330(2)	9.7038(4)	9.8562(3)
c (Å)	6.8849(2)	6.7784(3)	6.883(3)	6.7834(2)	7.2723(7)	7.2095(4)
Scan time	10 s	10 s	15 s	10 s	15 s	15 s
Effective transmission	0.851804-1	0.913099-1	0.880322-1	0.875734-1	0.501713-1	0.718448-1
R_{int} (-)						
before SADABS absorption correction	0.0513	0.0301	0.0323	0.0436	0.1235	0.0849
after SADABS absorption correction	0.0246	0.0178	0.0209	0.0206	0.0513	0.0265
Measured reflections	8991	9364	7127	7441	9866	10335
Unique reflections	477	486	477	488	520	536
Refined parameters	42	43	42	43	42	42
$R1, I > 4\sigma$, data	0.0195	0.0243	0.0167	0.0255	0.0172	0.0179
$R1$, all unique data	0.0198	0.0244	0.0168	0.0256	0.0198	0.0190
$wR2$	0.0500	0.0637	0.0450	0.0664	0.0397	0.0462
Largest difference peaks ($e^- \text{ Å}^{-3}$)	+0.50 -0.44	+0.71 -0.87	+0.42 -0.38	+0.87 -0.92	+0.68 -0.41	+0.74 -1.02
Goodness-of-Fit	1.204	1.128	1.142	1.134	1.115	1.078

TABLE 3. Positional parameters and equivalent isotropic U for U-Th-bearing apatite

Atom	x	y	z	U_{eq}	Occ.
Ca1					
UFAP	2/3	1/3	0.00103(9)	0.0106(2)	$\text{Ca}_{0.999(4)}$
UCIAP	2/3	1/3	-0.00328(11)	0.0142(3)	$\text{Ca}_{0.994(2)} \text{U}_{0.006(2)}$
ThFAP	2/3	1/3	0.00107(7)	0.0107(2)	$\text{Ca}_{0.999(1)}$
ThCIAP	2/3	1/3	-0.00277(11)	0.0140(3)	$\text{Ca}_{0.977(2)} \text{Th}_{0.023(2)}$
ThSrFAP	2/3	1/3	-0.00033(6)	0.0094(2)	$\text{Sr}_{0.993(3)} \text{Th}_{0.007(3)}$
ThSrCIAP	2/3	1/3	0.00078(6)	0.0113(2)	$\text{Sr}_{0.985(4)} \text{Th}_{0.015(4)}$
Ca2					
UFAP	0.24017(6)	0.00774(6)	1/4	0.0095(2)	$\text{Ca}_{0.986(1)} \text{U}_{0.014(1)}$
UCIAP	0.26005(8)	0.00142(8)	1/4	0.0148(3)	$\text{Ca}_{0.993(1)} \text{U}_{0.007(1)}$
ThFAP	0.24016(5)	0.00764(5)	1/4	0.0097(2)	$\text{Ca}_{0.987(1)} \text{Th}_{0.013(1)}$
ThCIAP	0.25881(8)	0.00047(8)	1/4	0.0153(3)	$\text{Ca}_{0.979(1)} \text{Th}_{0.021(1)}$
ThSrFAP	0.23996(4)	0.01438(4)	1/4	0.0084(2)	$\text{Sr}_{0.993(3)} \text{Th}_{0.007(3)}$
ThSrCIAP	0.24918(4)	0.01125(4)	1/4	0.0108(2)	$\text{Sr}_{0.990(3)} \text{Th}_{0.010(3)}$
P					
UFAP	0.39801(7)	0.36890(7)	1/4	0.0069(2)	$\text{P}_{1.00}$
UCIAP	0.40542(9)	0.37323(9)	1/4	0.0096(3)	$\text{P}_{1.00}$
ThFAP	0.39821(6)	0.36905(6)	1/4	0.0070(2)	$\text{P}_{1.00}$
ThCIAP	0.40536(9)	0.37319(10)	1/4	0.0089(3)	$\text{P}_{1.00}$
ThSrFAP	0.39959(11)	0.36885(11)	1/4	0.0071(3)	$\text{P}_{1.00}$
ThSrCIAP	0.40395(11)	0.37108(11)	1/4	0.0077(3)	$\text{P}_{1.00}$
O1					
UFAP	0.32526(23)	0.48389(21)	1/4	0.0116(4)	$\text{O}_{1.00}$
UCIAP	0.34065(32)	0.49037(29)	1/4	0.0176(5)	$\text{O}_{1.00}$
ThFAP	0.32574(20)	0.48427(19)	1/4	0.0115(3)	$\text{O}_{1.00}$
ThCIAP	0.34060(33)	0.49059(31)	1/4	0.0172(6)	$\text{O}_{1.00}$
ThSrFAP	0.33016(34)	0.48116(32)	1/4	0.0120(6)	$\text{O}_{1.00}$
ThSrCIAP	0.33493(36)	0.48113(34)	1/4	0.0135(6)	$\text{O}_{1.00}$
O2					
UFAP	0.41220(22)	0.53290(22)	1/4	0.0132(4)	$\text{O}_{1.00}$
UCIAP	0.40992(28)	0.53574(28)	1/4	0.0188(6)	$\text{O}_{1.00}$
ThFAP	0.41194(19)	0.53296(19)	1/4	0.0132(3)	$\text{O}_{1.00}$
ThCIAP	0.40870(29)	0.53581(29)	1/4	0.0179(6)	$\text{O}_{1.00}$
ThSrFAP	0.41769(32)	0.53599(32)	1/4	0.0129(6)	$\text{O}_{1.00}$
ThSrCIAP	0.41534(34)	0.53385(34)	1/4	0.0174(7)	$\text{O}_{1.00}$
O3					
UFAP	0.34137(17)	0.25685(15)	0.07060(20)	0.0153(3)	$\text{O}_{1.00}$
UCIAP	0.35246(26)	0.26527(22)	0.06718(30)	0.0261(5)	$\text{O}_{1.00}$
ThFAP	0.34132(15)	0.25680(13)	0.07044(17)	0.0154(3)	$\text{O}_{1.00}$
ThCIAP	0.35229(27)	0.26510(23)	0.06708(30)	0.0256(5)	$\text{O}_{1.00}$
ThSrFAP	0.34385(25)	0.26107(22)	0.07879(28)	0.0145(5)	$\text{O}_{1.00}$
ThSrCIAP	0.35395(29)	0.26649(25)	0.07678(32)	0.0208(5)	$\text{O}_{1.00}$
F					
UFAP	0	0	1/4	0.0220(7)	$\text{F}_{1.00}$
UCIAP	0	0	1/4	0.0220(6)	
ThFAP	0	0	1/4	0.0267(11)	$\text{F}_{1.00}$
ThCIAP					
ThSrFAP	0	0	1/4	0.0267(11)	$\text{F}_{1.00}$
ThSrCIAP					
Cl					
UFAP					
UCIAP	0	0	0.05948(95)	0.0688(28)	$\text{Cl}_{1.00}$
ThFAP	0	0	0.05940(101)	0.0689(30)	$\text{Cl}_{1.00}$
ThCIAP					
ThSrFAP	0	0	0	0.0247(5)	$\text{Cl}_{1.00}$
ThSrCIAP					

with digital signal processing (DSP) technology. UO_2 , uranyl nitrate, and uranyl acetate were used as U(IV) and U(VI) reference compounds. Spectra from the reference compounds were collected immediately before or after spectra from the samples. The data were processed using standard procedures utilizing the WinXAS 3.11 software package.

RESULTS

Chemical analysis

Chemical compositions of U- and Th-bearing fluor-, chlor-, and strontium-apatite were determined. Five individual spot analyses were taken on each sample. Table 1 reports the average of the best 3 spot analyses for each sample (with standard deviations ranging from 0.200 to 3.625), as well as the recalculated chemical formulae. For Th-doped chlorapatite (ThCIAP), the chemical composition is normalized to 100 wt% analytical totals. The use of only the best 3 spot analyses for each sample and normalization to 100% for ThCIAP is because of non-ideal data resulting from difficulties in preparation and quantitative analysis on relatively small sized samples. There are several experimental variables which can cause this, including the quality of polish and the overlap between the beam and epoxy surrounding the crystal, which can result in a low analytical total (Dunbar et al. 2003). The presence of minor amounts of F, Sr, and Th in U-doped chlorapatite (UCIAP) is probably attributable to contamination.

The EMPA results show that the average concentration of UO_2 is 2.00 wt% in UFAP and 1.03 wt% in UCIAP. The mean value of ThO_2 concentration is 1.79 wt% in ThFAP and 4.61 wt% in ThCIAP. For ThSrFAP and ThSrCIAP, the average ThO_2 concentrations are 1.67 and 0.01 wt%, respectively. Except for ThSrCIAP, these results from EMPA are consistent with the results from structure refinements of single-crystal diffraction data as described below. For ThSrCIAP, only one crystal was analyzed by EMPA, we speculate the inconsistency of Th content between EMPA and structure-refinement results is due to heterogeneity among different crystals in the same batch.

Structure refinements and site occupancies

As shown in Table 2, the synthetic apatite structures were refined to $R1 = 0.0167\text{--}0.0255$. Table 3 contains positional parameters, equivalent isotropic thermal parameters for U- and Th-bearing fluor-, chlor-, and strontium-apatite, and site occupancies. For each of the structure refinements (except those for the UFAP samples) the occupants of the Ca1 and Ca2 sites

TABLE 4. Selected bond lengths (Å)

	Natural F-apatite*	UFAP	ThFAP	Natural Cl-apatite*	UCIAP	ThCIAP	Pure Sr F-apatite†	ThSrFAP	Pure Sr Cl-apatite‡	ThSrCIAP
Ca1-O1 (x3)	2.399(2)	2.396(1)	2.396(1)	2.407(2)	2.408(2)	2.411(2)	2.544(6)	2.550(2)	2.567(2)	2.569(2)
O2 (x3)	2.457(2)	2.456(1)	2.455(1)	2.448(2)	2.447(2)	2.444(2)	2.572(2)	2.571(2)	2.580(2)	2.587(2)
O3 (x3)	2.807(2)	2.806(1)	2.806(1)	2.793(2)	2.797(2)	2.799(2)	2.895(7)	2.904(2)	2.859(2)	2.866(3)
Mean	2.554	2.553	2.552	2.549	2.551	2.551	2.670	2.675	2.669	2.674
Ca2-O1	2.701(2)	2.680(2)	2.683(2)	2.901(2)	2.910(3)	2.907(3)	2.731(10)	2.737(3)	2.847(2)	2.823(3)
O2	2.374(2)	2.382(2)	2.383(2)	2.306(2)	2.301(3)	2.314(3)	2.501(10)	2.492(3)	2.437(2)	2.433(3)
O3 (x2)	2.349(2)	2.351(1)	2.350(2)	2.331(2)	2.323(2)	2.323(2)	2.519(8)	2.517(2)	2.510(2)	2.504(2)
O3 (x2)	2.501(2)	2.494(1)	2.494(1)	2.544(2)	2.552(2)	2.560(2)	2.646(7)	2.649(2)	2.696(2)	2.701(2)
Ca2-F	2.3108(7)	2.2871(4)	2.2882(7)	—	—	—	2.394(1)	2.4014(3)	—	—
Ca2-Cl	—	—	—	2.759(1)	2.810(3)	2.806(3)	—	—	3.086(1)	3.0927(3)
Mean	2.441	2.434	2.435	2.531	2.539	2.542	2.565	2.566	2.683	2.680
P-O1	1.537(3)	1.537(2)	1.537(2)	1.533(3)	1.537(2)	1.541(3)	1.542(9)	1.541(3)	1.540(2)	1.542(3)
O2	1.539(3)	1.540(2)	1.542(2)	1.538(3)	1.545(3)	1.551(3)	1.521(10)	1.536(3)	1.544(2)	1.543(3)
O3 (x2)	1.532(3)	1.533(1)	1.536(1)	1.524(2)	1.532(2)	1.534(2)	1.532(8)	1.540(2)	1.537(2)	1.535(2)
Mean	1.535	1.537	1.538	1.530	1.538	1.540	1.532	1.539	1.540	1.540

* Data from Hughes et al. (1989).

† Data from Swafford and Holt (2002).

‡ Data from Sudarsanan and Young (1974).

were refined with the constraint of actinide (U or Th) + Ca = 1. As the U-doped fluorapatite (UFAP) is the only sample containing Na in its starting reagents, following the procedure of Hughes et al. (1991), we assigned a partial occupancy of Na only on the Ca1 site (equal to the analyzed amount of Na) to provide a limiting case for U ordering. Thus the amount of U in the Ca2 site represents a minimum, i.e., if any Na resides on Ca2 then the U concentration will be higher than that refined. The occupants of the Ca2 site were refined with the constraint of U + Ca = 1 in UFAP.

The results for the U-doped fluorapatites indicate that U partitions almost exclusively into the Ca2 site. Values of $U_{\text{Ca}2}/U_{\text{Ca}1}$, calculated per individual site normalized by the multiplicity of that site, range from 5.00 to 9.33. Similarly, structure refinements of Th-doped fluorapatite specimens indicate that Th substitutes dominantly into the Ca2 site with $\text{Th}_{\text{Ca}2}/\text{Th}_{\text{Ca}1}$ values that range of 4.33 to 8.67. For U-doped chlorapatite U is essentially equally distributed between the two Ca sites with $U_{\text{Ca}2}/U_{\text{Ca}1}$ values that range from 0.89 to 1.17. For the Th-doped chlorapatite Th substitutes into both Ca1 and Ca2 sites with $\text{Th}_{\text{Ca}2}/\text{Th}_{\text{Ca}1}$ values that range from 0.61 to 0.67. In the Th-doped strontium-apatites with F and Cl end-members, Th is incorporated in both Ca1 and Ca2 sites. The range of $\text{Th}_{\text{Ca}2}/\text{Th}_{\text{Ca}1}$ values is 0.56 to 1.00 for the F end-member, and 0.39 to 0.94 for the Cl end-member. The concentration of actinide (U or Th) in each sample, determined in the refinement, is 2.09 wt% U in UFAP, 2.02 wt% U in UCIAP, 1.89 wt% Th in ThFAP, 4.71 wt% Th in ThCIAP, 1.24 wt% Th in ThSrFAP, and 1.81 wt% Th in ThSrCIAP. Based on the Th content determined by the structure refinements, it appears that the chlorapatite structure is capable of accommodating a larger amount of Th than its fluorapatite counterpart (i.e., 4.71 wt% Th in ThCIAP vs. 1.89 wt% in ThFAP). The same is true in strontium-apatites (i.e., 1.81 wt% Th in ThSrCIAP vs. 1.24 wt% Th on ThSrFAP). This is speculative, however, because the heterogeneity in the actinide concentration among crystals in a single sample was not thoroughly investigated.

Bond-length variations

Table 4 shows a comparison of selected bond lengths for natural fluor-, chlorapatite crystals (Hughes et al. 1989), synthetic U- and Th-doped fluor- and chlorapatite, synthetic Th-doped

strontium fluor-, chlorapatite, and pure synthetic strontium fluor-, chlorapatite (Swafford and Holt 2002; Sudarsanan and Young 1974). The average bond length in each of the Ca sites shows that in the U- and Th-doped fluor- and chlorapatite crystals, Ca1-O distances are not affected by the substitution of U or Th. However, Ca2-O distances are affected by both cation and anion substitutions, and thus variations at the Ca2 site are not regular among the different apatite species. The mean bond length for Ca2 in fluorapatite decreases from 2.441 to 2.434 Å with U substitution and from 2.441 to 2.435 Å with Th substitution. However, in chlorapatite the mean Ca2 bond lengths increase from 2.531 to 2.539 Å on substitution of U for Ca, and from 2.531 to 2.542 Å due to the substitution of Th. These significant changes due to U/Th substitution are unusual and are discussed below. There are also variations in the mean bond distances of the tetrahedral site among the samples, which reflect differences in the substitution of Si for P. For all of the U- and Th-doped fluor-, chlorapatite specimens, the mean tetrahedral bond distances range from 1.537 to 1.540 Å, in comparison to 1.530 and 1.535 Å for natural fluorapatite and chlorapatite, respectively. For Th-doped strontium fluor- and chlorapatite, the mean bond lengths for both the Sr1 and Sr2 sites show only a slight increase from 0.001 to 0.005 Å relative to pure strontium fluor- and chlorapatite.

Uranium oxidation state

Unlike Th, U has two common oxidation states that exist in the natural environment, U^{4+} and U^{6+} . The most important characteristic of uranium regarding its mobility is that U^{4+} is very insoluble, whereas U^{6+} is much more soluble in natural waters (Renshaw et al. 2005). To use apatite as a solid nuclear waste form and engineered contaminant barrier for U, it is important to know the oxidation state of U in the apatite structure and its relationship to site occupancy and structure distortions.

The XANES spectra of the U-doped fluorapatite (UFAP) and U-doped chlorapatite (UCIAP), together with those of the U^{4+} and U^{6+} reference compounds, are shown in Figure 2. Uranium in fluorapatite exists as U^{4+} , as evidenced by the absorption edge position of U in fluorapatite relative to U^{4+} and U^{6+} standards (Fig. 2a). Among our standards, UO_2 and uranyl nitrate are powder samples mixed with BN, which are not ideal for micro-beam

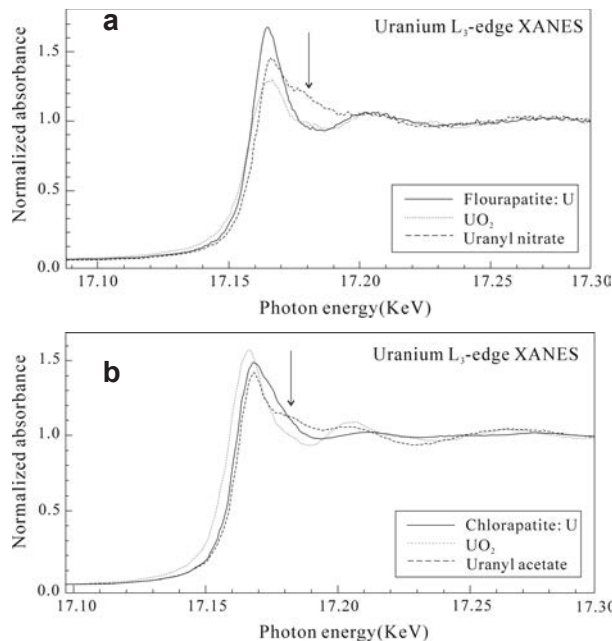


FIGURE 2. Room-temperature uranium L_3 -edge XANES measurements on synthetic fluorapatite and chlorapatite together with standards. (a) U in fluorapatite with U^{4+} [UO_2] and U^{6+} [uranyl nitrate] standards. (b) U in chlorapatite with U^{4+} [UO_2] and U^{6+} [uranyl acetate] standards. The arrows indicate the position of the postedge MSR feature associated with U^{6+} .

fluorescence measurements. In Figure 2a, the intensity of the white line of the standards is suppressed due to self-absorption. However, because self-absorption has a negligible effect on the measured edge position the comparison here is still legitimate. Furthermore, the absence of post-edge multiple scattering resonance (MSR) features, such as a “shoulder,” which are usually observed in U^{6+} XANES spectra (Bertsch et al. 1994; Hunter and Bertsch 1998; Duff et al. 2000), also indicates that U is tetravalent in fluorapatite. The absorption edge position of U in chlorapatite (Fig. 2b) indicates that U exists as a combination of both U^{4+} and U^{6+} . The position of the edge shows that most U in chlorapatite is hexavalent. The displacement of the absorption edge toward the UO_2 edge and the shallow post edge slope instead of the MSR “shoulder” indicates there is tetravalent U in this sample as well. Bertsch et al. (1994) found a linear relationship ($r^2 = 0.987$) between the proportional amounts of U^{4+} and U^{6+} in physical admixtures of uranium compounds and the central location of the edge position. Using this relationship and the edge position, determined by the inflection point of the absorption edge, roughly 20% U in chlorapatite is U^{4+} , whereas about 80% is U^{6+} .

In comparison with our finding that U^{4+} substitutes into the Ca2 site in fluorapatite, Rakovan et al. (2002) found U^{6+} almost exclusively substitutes into the Ca1 site of fluorapatite. If the U concentration in the two Ca sites of the chlorapatite is normalized by the multiplicity of the sites ($0.80 \text{ wt\%}/4 = 0.2 \text{ wt\%}$ for Ca1 and $1.22 \text{ wt\%}/6 = 0.2 \text{ wt\%}$ for Ca2), we find that U is essentially equally distributed between these sites. Also, based on the X-ray absorption edge position, it is estimated that roughly 80% of the U is U^{6+} in chlorapatite. Thus assuming all U^{4+} substitutes

into Ca2 site, to account for the equal distribution of U between Ca1 and Ca2 in chlorapatite, at least 37% of the U^{6+} must also substitute into Ca2 site. The discrepancy between this result and that of Rakovan et al. (2002) may be due to different synthesis methods as well as the structure variation caused by different anion components as described below.

DISCUSSION

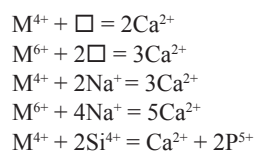
The crystal chemical factors that determine site preference of U and Th in apatite are complex, and include radius constraints, substitution mechanisms, bond valence, and the structure variations caused by the substitutions. These factors are discussed in turn below.

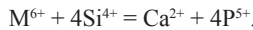
Radius constraints

According to Shannon (1976), the effective ionic radius for Ca is 1.18 Å in ninefold coordination, and 1.06 Å in sevenfold coordination. The ionic radius for Th^{4+} is 1.09 and ~1.03 Å in ninefold and sevenfold coordination respectively. The ionic radius for U^{4+} is 1.05 Å in ninefold coordination and 0.87 Å in sevenfold coordination, and the ionic radius for U^{6+} is 0.86 Å in ninefold coordination and 0.73 Å in sevenfold coordination. As Th^{4+} , U^{4+} , and U^{6+} are smaller than Ca^{2+} , ionic radii alone suggest that these three ions can substitute into either Ca site in the apatite structure. The coordination number is nine for the Ca1 site and seven for the Ca2 site (Fig. 1). Elliott (1994) pointed out that this difference has been used to suggest that purely on the basis of size, the Ca1 site should be occupied preferentially by ions larger than Ca^{2+} . Based on this argument, Th^{4+} , U^{4+} , and U^{6+} should preferentially occupy the smaller Ca2 site. This is not consistent with our results, however, which indicate that U^{4+} and Th^{4+} substitute into Ca2 site in fluorapatite but into both Ca1 and Ca2 sites in chlorapatite. Thus, radius constraints alone cannot explain the distribution of U and Th between the two Ca sites in apatite.

Substitution mechanism

Because both U and Th have greater positive charges than Ca^{2+} , for which they substitute in apatite, a coupled substitution is necessary to maintain charge balance. Several studies have indicated that U and Th can substitute for Ca via a Ca-deficiency mechanism such as vacancies (Hughson and Gupta 1964; Baumer et al. 1983; Clarke and Altschuler 1958). In addition, various coupled substitutions involving Na, Si, and vacancies have been shown for trivalent and tetravalent cation substitutions for Ca in apatite (Pan and Fleet 2002). As noted in the EMPA analysis, Na was present in the starting materials for sample UFAP and Si was in the starting materials of all the Ca apatites. Based on the chemical analyses of U-, Th-doped fluor-, chlor-, and strontium-apatite specimens in this study, local charge compensation may be maintained by the following coupled substitutions (M represents U or Th, □ represents vacancy):





Several studies described the substitution mechanism as a control on partitioning of REEs between the two Ca sites in apatite (Fleet and Pan 1995, 1997; Mackie and Young 1973). According to Fleet and Pan (1995), the substitution of REEs for Ca is charge compensated by Na in ClAp, Na and Si in FAp, and Si in OHAp. It is unclear, however, if the various partitioning schemes of U and Th in fluorapatite and chlorapatite in this study are directly or indirectly related to these substitution mechanisms.

Bond valence

In addition to charge compensation, bond valence must be met in the substitution of the U or Th for Ca. Table 5 gives the bond valence sum for U and Th in the Ca sites of analyzed apatites. The preferred sites indicated by bond valence are bold and italic. The sites that U or Th actually substitute into are indicated by the asterisk. Surprisingly, site occupancies predicted by bond valence are not consistent with our measurements. In fluorapatite, U and Th are less underbonded in the Ca1 site than in the Ca2 site. Thus, based on bond valence considerations, they should prefer the Ca1 site, assuming no structural response to accommodate the substitution. However, our results show a marked preference of U^{4+} and Th^{4+} for the Ca2 site. Similarly, bond valence calculations indicate that both U and Th are less underbonded in the Ca1 site in chlorapatite, yet our results indicate that they substitute into both Ca sites equally in chlorapatite. Also, the bond valence for Th in strontium fluorapatite and chlorapatite suggests that Th should substitute into Ca1 site whereas our results indicate it substitutes into both Ca sites with $\text{Th}_{\text{Ca}2}/\text{Th}_{\text{Ca}1}$ ratios that range from 0.39 to 1.00. Fleet and Pan (1995) pointed out that bond valence calculations are based on the correlation between bond distance and bond strength and therefore also embody a component attributed to variation in the size of structural positions. This coupling of the effects of bond valence and substituent size gives rise to an ambiguity in interpretation. As discussed below, the structure variations of single crystal apatites may contribute to the ambiguity of bond valence interpretation in our case.

Structure variations

The volume of each Ca polyhedron was calculated using program VOLCAL (Hazen and Finger 1982). The results (Fig. 3) show that the volume of the Ca2 polyhedron increases from 21.68 \AA^3 in fluorapatite to 22.94 \AA^3 in chlorapatite (5.8%). In contrast, the Ca1 polyhedron increases from 31.92 \AA^3 in fluorapatite to 32.11 \AA^3 in chlorapatite (0.59%). The replacement of F by a Cl⁻ ion affects the Ca2 polyhedron much more than Ca1 polyhedron. Similar to the conclusion of Fleet et al. (2000) on REEs in Cl-apatite, we suggest the preference of both Ca sites of U and Th in chlorapatite is related to the large increase in size and distortion of the Ca2 polyhedron upon substitution of Cl for F. The much larger size of Ca2 in chlorapatite may diminish the selectivity of this position for U and Th.

It is difficult to generalize what controls the distribution of U and Th between the two Ca sites in the apatite structure. Because the radius constraint, the charge balance, and the bond valence equalization together cannot account for the site preference of U

and Th in apatite, we speculate that the volatile anion component might be a significant factor in the selectivity of apatite for U and Th because of its marked influence on the stereochemical environment and effective size of the Ca2 site.

Figure 3 also shows that the incorporation of U and Th into fluorapatite results in a decrease in the size of both Ca polyhedra, but the incorporation of U and Th into chlorapatite gives rise to an increase in the volume of both Ca polyhedra. The decrease of both Ca polyhedral volumes in fluorapatite caused by the substitution of U and Th can be explained by the decrease of ionic radius from Ca to U and Th. However, the increase in the

TABLE 5. Bond valences calculated for U and Th in Ca1 and Ca2 sites in apatite

	FAP	CIAP	UFAP	UCIAP	ThFAP	ThCIAP	ThSrFAP	ThSrCIAP
Ca1	2.04	2.05	3.03	3.03*	3.53	3.52*	2.45*	2.43*
Ca2	1.94	2.00	2.96*	2.88*	3.40*	3.31*	2.33*	2.16*

Notes: The preferred site indicated by bond valence calculation are bold and italic. The sites that U and Th actually substitute into are indicated by the asterisk.

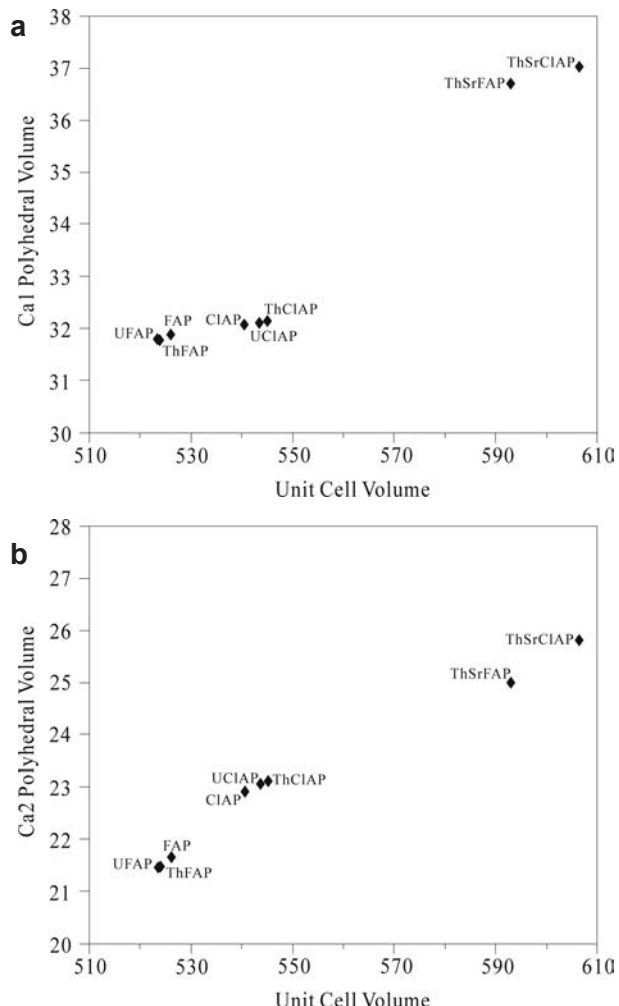


FIGURE 3. Variation in volume (\AA^3) of the Ca1O_9 polyhedron (a) and the $\text{Ca}_2\text{O}_6\text{X}$ polyhedron (b) with unit-cell volume for natural F-, Cl- apatite, synthetic UFAP, ThFAP, and ThClFAP. Polyhedral volumes were calculated with VOLCAL.

volume of both Ca polyhedra in chlorapatite is hard to understand. Because of the effect on Ca2 polyhedron caused by the replacement of F⁻ by Cl⁻, we suggest it is due to the structural distortion of Ca2 polyhedron.

ACKNOWLEDGMENTS

This work was supported by NSF grants EAR-0409435 and EAR-0003201. We thank James Ablett and Paul Northrup at beamline X27A, NSLS for their help for setting up our XANES experiments. William Lack and Barry Landrum of the Miami Instrumentation Laboratory are gratefully acknowledged for maintaining the X-ray instrumentation and building our experimental goniometer used for XANES data collection.

REFERENCES CITED

- Altschuler, Z.S., Clarke Jr., R.S., and Young, E.J. (1958) Geochemistry of uranium in apatite and phosphorite. Geological Survey Professional Paper, 314-D, 45–90.
- Baumer, A., Caruba, R., Bizouard, H., and Peckett, A. (1983) Synthetic chlorapatite: Substitution and inclusion of trace quantities of manganese, cerium, uranium and thorium. Canadian Mineralogist, 21, 567–573.
- Bertsch, P.M., Bajt, S., Hunter, D.B., Rivers, M.L., and Sutton, S.R. (1994) In situ chemical speciation of uranium in soils and sediments by micro X-ray absorption spectroscopy. Environmental Science and Technology, 28, 980–984.
- Bostick, W.D., Jarabek, R.J., Bostick, D.A., and Conca, J.L. (1999) Phosphate-induced metal stabilization: use of apatite and bone char for the removal of soluble radionuclides in authentic and simulated DOE groundwater. Advances in Environmental Research, 3, 488–498.
- Bruker (1997) SADABS, SAINT, SMART, and SHELLXTL. Bruker AXS Inc., Madison, Wisconsin.
- Carpena, J. and Lacout, J.L. (1998) Process for the conditioning of radioactive waste using phosphosilicate apatites as the confinement matrix. U.S. Patent 5771472. U.S. Patent and Trademark Office, Alexandria, Virginia.
- Carpena, J., Boyer, L., and Lacout, J.L. (2003) Method to confine plutonium in apatitic ceramics and products obtained using said process. U.S. Patent 6624339. U.S. Patent and Trademark Office, Alexandria, Virginia.
- Chen, X., Wright, J., Conca, J.L., and Peurung, L.M. (1997a) Effects of pH on heavy metal sorption on mineral apatite. Environmental Science and Technology, 31, 624–631.
- (1997b) Evaluation of heavy metal remediation using mineral apatite. Water, Air, and Soil Pollution, 98, 57–78.
- Clarke Jr., R.S. and Altschuler, Z.S. (1958) Determination of the oxidation state of uranium in apatite and phosphorite deposits. Geochimica et Cosmochimica Acta, 13, 127–142.
- Conca, J.L. and Wright, J.V. (1998) PIMS: A simple technology for clean-up of heavy metals and radionuclides throughout the world. In T.E. Baca, Ed., The Environmental Challenges of Nuclear Disarmament: Proceedings of the NATO Advanced Research Workshop, Cracow, Poland, 9–13 November, 1998, p. 1–13. Springer, New York.
- Conca, J.L., Jambor, J.L., and Wright, J. (2006) An apatite II permeable reactive barrier to remediate ground water containing Zn, Pb, and Cd. Applied Geochimistry, 21, 1288–1300.
- Della Ventura, G., Bellatreccia, F., Cabella, R., Caprilli, E., Oberti, R., and Williams, C.T. (1999) Britholite–hellandite intergrowths and associated REE-minerals from the alkali-syenitic ejecta of the Vico volcanic complex (Latium, Italy): Petrological implications bearing on REE mobility in volcanic systems. European Journal of Mineralogy, 11, 843–854.
- Dunbar, N.W., Zielinski, G.A., and Voisins, D.T. (2003) Tephra layers in the Siple dome and Taylor dome ice cores, Antarctica: Sources and correlations. Journal of Geophysical Research, 108(B8), 2374, DOI: 10.1029/2002JB002056.
- Duff, M.C., Bertsch, P.M., Hunter, D.B., and Morris, D.E. (2000) Spectroscopic characterization of uranium in evaporation basin sediments. Geochimica et Cosmochimica Acta, 64, 1535–1550.
- Elliott, J.C. (1994) Structure and Chemistry of the Apatites and Other Calcium Orthophosphates. Elsevier, New York.
- Ewing, R.C. and Wang, L. (2002) Phosphates as nuclear waste forms. In M.J. Kohn, J. Rakovan, and J.M. Hughes, Eds., Phosphates—Geochemical, Geobiological, and Materials Importance, 48, p. 673–699. Reviews in Mineralogy and Geochemistry, Mineralogical Society of America, Chantilly, Virginia.
- Fleet, M.E. and Pan, Y. (1995) Site preference of rare earth elements in fluorapatite. American Mineralogist, 80, 329–335.
- (1997) Site preference of rare earth elements in fluorapatite: Binary (LREE + HREE)-substituted crystals. American Mineralogist, 82, 870–877.
- Fleet, M.E., Liu, X., and Pan, Y. (2000) Rare-earth elements in chlorapatite [Ca₁₀(PO₄)₆Cl₂]: Uptake, site preference, and degradation of monoclinic structure. American Mineralogist, 85, 1437–1446.
- Hazen, R.M. and Finger, L.W. (1982) Comparative crystal chemistry: Temperature, pressure, composition, and the variation of crystal structure. Wiley, New York.
- Hughes, J.M. and Rakovan, J. (2002) The crystal structure of apatite, Ca₅(PO₄)₃(F,OH,Cl). In M.J. Kohn, J. Rakovan, and J.M. Hughes, Eds., Phosphates—Geochemical, Geobiological, and Materials Importance, 48, p. 1–12. Reviews in Mineralogy and Geochemistry, Mineralogical Society of America, Chantilly, Virginia.
- Hughes, J.M., Cameron, M., and Crowley, K.D. (1989) Structural variations in natural F, OH, and Cl apatites. American Mineralogist, 74, 870–876.
- Hughes, J.M., Cameron, M., and Mariano, A.N. (1991) Rare-earth-element ordering and structural variations in natural rare-earth-bearing apatites. American Mineralogist, 76, 1165–1173.
- Hughson, M.R. and Gupta, J.G.S. (1964) A thorian intermediate member of the britholite-apatite series. American Mineralogist, 49, 937–951.
- Hunter, D.B. and Bertsch, P.M. (1998) In situ examination of uranium contaminated soil particles by micro-X-ray absorption and micro-fluorescence spectroscopies. Journal of Radioanalytical and Nuclear Chemistry, 234, 237–242.
- Knox, A.S., Adriano, D.C., Hinton, T.G., Kaplan, D.I., and Wilson, M.D. (2003) Apatite and phillipsite as sequestering agents for metals and radionuclides. Journal of Environmental Quality, 32, 515–525.
- Larsen Jr., E.S., Harrison, H.C., and Keevil, N.B. (1952) Method for determining the age of igneous rocks using the accessory minerals. Geological Society of America Bulletin, 63, 1045–1052.
- Mackie, P.E. and Young, R.A. (1973) Location of Nd dopant in fluorapatite, Ca₅(PO₄)₃F: Nd. Journal of Applied Crystallography, 6, 26–31.
- Mehmel, M. (1930) Über die struktur des apatits. Zeitschrift für Kristallographie, 75, 323–331.
- Náray-Szabó, S. (1930) The structure of apatite (CaF)Ca₄(PO₄)₃. Zeitschrift für Kristallographie, 75, 387–398.
- Nokhrin, S.M., Pan, Y., Weil, J.A., and Nilges, M.J. (2005) Multifrequency EPR study of radiation-damage-induced defect centers in chlorapatite. Canadian Mineralogist, 43, 1581–1588.
- Oberti, R., Della Ventura, G., Ottolini, L., and Parodi, G.C. (2001) On the symmetry and crystal chemistry of britholite: new structural and microanalytical data. American Mineralogist, 86, 1066–1075.
- Oosthuizen, E.J. and Burger, A.J. (1973) The suitability of apatite as an age indicator by the uranium–lead isotope method. Earth and Planetary Science Letters, 18, 29–36.
- Pan, Y. and Fleet, M.E. (2002) Compositions of the apatite group minerals: Substitution mechanisms and controlling factors. In M.J. Kohn, J. Rakovan, and J.M. Hughes, Eds., Phosphates—Geochemical, Geobiological, and Materials Importance, 48, p. 13–49. Reviews in Mineralogy and Geochemistry, Mineralogical Society of America, Chantilly, Virginia.
- Pan, Y., Dong, P., and Chen, N. (2003) Non-Henry's Law behavior of REE partitioning between fluorapatite and CaF₂-rich melts: Controls of intrinsic vacancies and implications for natural apatites. Geochimica et Cosmochimica Acta, 67, 1889–2003.
- Prener, J.S. (1967) The growth and crystallographic properties of calcium fluor- and chlorapatite crystals. Journal of the Electrochemical Society, 114, 77–83.
- Raicevic, S., Wright, J.V., Veljkovic, V., and Conca, J.L. (2006) Theoretical stability assessment of uranyl phosphates and apatites: Selection of amendments for in situ remediation of uranium. Science of the Total Environment, 355, 13–24.
- Rakovan, J., Reeder, R.J., Elzinga, E.J., Cherniak, D.J., Tait, C.D., and Morris, D.E. (2002) Structural characterization of U(VI) in apatite by X-ray absorption spectroscopy. Environmental Science and Technology, 36, 3114–3117.
- Renshaw, J.C., Butchins, Laura J.C., Livens, F.R., May, I., Charnock, J.M., and Lloyd, J.R. (2005) Bioreduction of uranium: Environmental implications of a pentavalent intermediate. Environmental Science and Technology, 39, 5657–5660.
- Shannon, R.D. (1976) Revised effective ionic radii and systematic studies of interatomic distances in halides and chalcogenides. Acta Crystallographica, A32, 751–761.
- Sudarsanan, K. and Young, R.A. (1974) Structure refinement and random error analysis for strontium “chlorapatite,” Sr₅(PO₄)₃Cl. Acta Crystallographica, B30, 1381–1386.
- Swafford, S.H. and Holt, E.M. (2002) New synthetic approaches to monophosphate fluoride ceramics: Synthesis and structural characterization of Na₂Mg(PO₄)F and Sr₅(PO₄)₃F. Solid State Sciences, 4, 807–812.

MANUSCRIPT RECEIVED MAY 25, 2008

MANUSCRIPT ACCEPTED SEPTEMBER 10, 2008

MANUSCRIPT HANDLED BY G. DIEGO GATTA